Available online at www.sciencedirect.com
ScienceDirect
Bioorganic & Medicinal Chemistry 15 (2007) 1439–1447
Bioorganic & Medicinal Chemistry

High affinity Grb2-SH3 domain ligand incorporating C^{β}-substituted prolines in a Sos-derived decapeptide

Yves Jacquot,[a,*] Isabelle Broutin,[b] Emeric Miclet,[a] Magali Nicaise,[c] Olivier Lequin,[a] Nicole Goasdoué,[a] Charlotte Joss,[a] Philippe Karoyan,[a] Michel Desmadril,[c] Arnaud Ducruix[b] and Solange Lavielle[a]

[a]*Université Pierre et Marie Curie-Paris 6, UMR 7613, Paris, France; CNRS, UMR 7613, ''Synthèse, Structure et Fonction de Molécules Bioactives'', Paris, France; FR 2769, UMR 7613, Paris, France; Case courrier 45, 4, place Jussieu, 75005 Paris, France*
[b]*Université René Descartes, UMR 8015, Paris, France; CNRS, UMR 8015, Laboratoire de Cristallographie et RMN biologique, Paris, France; 4, avenue de l'Observatoire, 75270 Paris Cedex 06, France*
[c]*Université de Paris-Sud, UMR 8619, Orsay, France; CNRS, UMR 8619, Laboratoire de Modélisation et d'Ingénierie des Protéines, Orsay, France; Bât. 430, 91405 Orsay Cedex, France*

Received 10 July 2006; revised 30 October 2006; accepted 2 November 2006
Available online 6 November 2006

Abstract—Peptide ligands that disrupt MAPK pathways are of great interest for a better understanding of these signalling cascades and represent therefore an attractive target to control cell degenerative processes. In that context, selective disruption of the upstream Grb2/Sos complex in the Ras/MAPK cascade has focused extensive work. The Sos PPII decapeptide, which interacts with the Grb2-SH3 domains, has been modified in various positions and the best inhibitors designed so far are either dimeric ligands or peptoid analogues of the VPPPVPPRRR sequence. We report the synthesis of new Grb2 ligands in which the key Val5 residue has been replaced by a *cis* C^{β}-substituted proline. Both fluorescence and ITC assays have been employed to measure the affinity of these substituted peptides for a recombinant Grb2 protein. Whereas proline in position 5 completely abolished the binding potency, a *cis* C^{β}-methyl-L-proline restored the affinity. Other *cis* C^{β}-proline substituents led to a complete loss of binding potency. Combining the best modifications: a *cis* C^{β}-methylproline 5, *N*-acetylation, C-carboxamide and dimerization yielded a 560-fold affinity enhancement compared to the wild-type VPPPVPPRRR sequence. This study shows that C^{β}-substituted prolines may constitute a new alternative for PPII ligands, combining entropy and enthalpy beneficial effects.

1. Introduction

Growth factors are involved in many biological processes such as differentiation, survival, apoptosis as well as cytoskeleton reorganisation via interactions with their specific tyrosine kinase receptor (TKR), which activates the Ras/MAPK cascade.[1–3] This signalling pathway has been highlighted as mutations in the Ras protein have been found in human carcinoma suggesting a crucial role of Ras in cell degenerative processes and cancer emergence.[4] Stimulation by a growth factor of TKR induces first dimerization followed by autophosphorylation of the receptor and the recruitment of the Grb2/Sos complex. This latter complex is stabilized mainly by hydrophobic interactions between the two SH3 domains of Grb2 and the decapeptide Val1149-Arg1158 (VPPPVPPRRR) from Sos.[5,6] NMR structure of the N-terminal Grb2-SH3 domain/VPPPVPPRRR complex[7,8] showed that this decapeptide adopts a polypro-

Abbreviations: MAPK, mitogen-activated protein kinase; Grb2, growth factor receptor-bound protein 2; SH3, Src homology 3; PPII, polyproline II; Sos, son of sevenless; CD, circular dichroism; TKR, tyrosine kinase receptor; NMR, nuclear magnetic resonance; Boc, *tert*-butyloxycarbonyl; Fmoc, 9-fluorenylmethoxycarbonyl; ITC, isothermal titration calorimetry; Tos, tosylate; PAM, phenylacetamidomethyl resin; MBHA, 4-methylbenzhydrylamine resin; DCC, dicyclohexylcarbodiimide; HOBt, hydroxybenzotriazole; HBTU, *O*-(1*H*-benzotriazol-1-yl)-1,1,3,3-tetramethyluronium hexafluorophosphate; DMSO, dimethylsulfoxide; DMPU, 1,3-dimethyl-3,4,5,6-tetrahydro-2-(1*H*)-pyrimidinone; HEPES, 4-(2-hydroxyethyl)-1-piperazineethane sulfonic acid; RP-HPLC, reverse-phase high performance liquid chromatography; MALDI-TOF, matrix-assisted laser desorption ionization time-of-flight; TFA, trifluoroacetic acid; NMP, *N*-methylpyrrolidone; DIEA, *N*,*N*-diisopropylethylamine; Standard IUPAC single and triple letter codes for amino acids are used.

Keywords: Grb2-SH3 domain; C^{β}-substituted prolines; Fluorescence; ITC.

* Corresponding author. Tel.: +33 (0)1 44 27 26 78; fax: +33 01 44 27 38 43; e-mail: jacquot@ccr.jussieu.fr

0968-0896/$ - see front matter © 2006 Elsevier Ltd. All rights reserved.
doi:10.1016/j.bmc.2006.11.002

line II (PPII) helical conformation, i.e. a left-handed helix with three residues per turn ($\phi = -78°$, $\psi = +146°$).[9] This VPPPVPPRRR sequence belongs to the proline-rich domains superfamily, which represents the most important protein interaction modules whose prominent feature is their ability to form weak complexes with specific recognizing domains, their dissociation constants being typically in the micromolar range.[10,11]

Selective disruption of the Grb2/Sos association has been considered as an attractive strategy for an upstream control of the Ras/MAPK cascade.[3,12] Two families of ligands have emerged to provide inhibitors of this protein/protein interaction: (i) PPII ligand dimers, which allow simultaneous interaction with both Grb2-SH3 domains[13] and (ii) peptoids, which establish new stabilizing interactions with the Grb2 protein.[10,14] However, the selectivity of these ligands remains an important question to be addressed,[11,15,16] since more than two hundred SH3 domains have been identified or suspected in mammals.[17] In that context, we have designed analogues of the decapeptide VPPPVPPRRR incorporating a C^{β}-substituted proline in place of the crucial valine 5 residue, as an application of the chimeric prolinoamino acids (Fig. 1) previously described.[18–24] Indeed, close disclosure of the Grb2/SH3 binding surface showed that the central valine side chain (Val5) of ^{1}VPPPVPPRRR[10] is located in a hydrophobic groove (Fig. 2), and constitutes a strategic position to anchor the decapeptide within the Grb2 protein. Furthermore, this Val5 residue is located between the two prolines Pro3 and Pro6, which have been replaced by either an alanine or a sarcosine by Nguyen et al.[10] Since *N*-alkylation (sarcosine and peptoids) is advantageously accepted in position 6, we reasoned that (i) a C^{β}-substituted proline in position 5 might project the β-substituent in the same direction as an *N*-alkylated residue in position 6 (enthalpy gain) and (ii) the ϕ-constraint of the proline ring in position 5 will stabilize and thus increase the concentration of the necessary PPII structure (entropy gain). Both gains should lead to high affinity binders of the Grb2 protein (Fig. 3). Thus, in the present study, Val5 has been replaced by various *cis* C^{β}-substituted-L-prolines. [18–24]

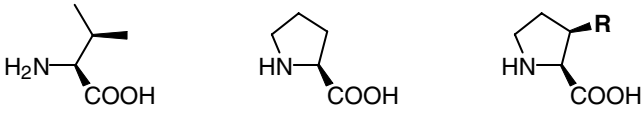

Figure 1. Structures of L-valine, L-proline and of the chimeric *cis* prolinoamino acid.

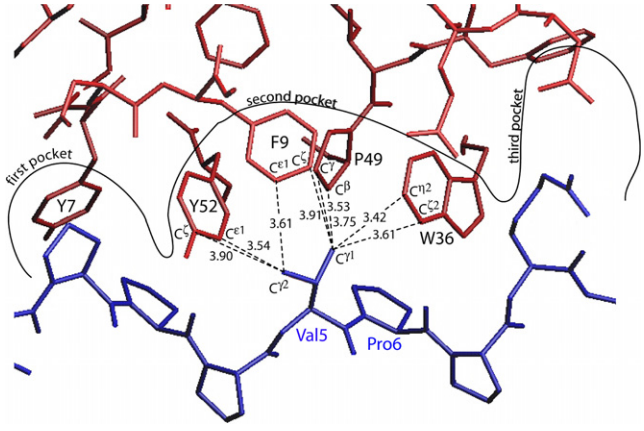

Figure 2. Interaction of the VPPPVPPRRR sequence of Sos (blue) with the N-terminal SH3 domain of Grb2 (red). Distances between the Val5 residue of Sos and the residues that constitute the aromatic-rich second pocket of the N-terminal SH3 domain of Grb2 are specified (PDB code 1GBQ[8]).

We report herein the syntheses of: (1) *N*-Fmoc or *N*-Boc aromatic, aliphatic-alkyl and polar *cis* C^{β}-substituted prolines, and (2) the corresponding peptides. The affinity of each peptide for recombinant Grb2 has been determined using fluorescence spectroscopy and/or ITC studies. Far-UV CD spectra have also been recorded for some representative peptides.

2. Results

2.1. C^{β}-substituted prolines and peptide syntheses

Syntheses of *N*-Fmoc or *N*-Boc *cis* C^{β}-substituted-L-prolines (Table 1) were based on the asymmetric amino-zinc-enolate carbometallation strategy, as we previously reported (Figs. 4 and 5).[18–24]

Most of the monomeric peptides reported herein are free amino and free carboxylic derivatives to allow direct comparison with previously reported studies.[13,25] They were prepared starting from preloaded Arg(-Tos)-PAM resin by manual or automatic solid phase peptide strategy with either DCC/HOBt or HBTU for the coupling of the hindered modified prolines (residue 5) and the following amino acid (residue 4). For the C-terminal carboxamide peptide **20** a MBHA resin and the Boc strategy were used, while the peptide dimer **21** was obtained from a preloaded Boc-Lys(Fmoc)-MBHA resin. Acetylation of the N-terminal residue of peptides **20** and **21** was achieved with acetic anhydride.

2.2. Monomers binding assays

Dissociation constants (K_d) of Grb2-SH3 domain/peptide complex were measured for each peptide by fluorescence spectroscopy and are listed in Table 2. For the wild-type Sos decapeptide VPPPVPPRRR (peptide **12**) a K_d of 38.7 ± 1.5 μM was determined. No significant binding affinity was detected for VPPPPPPRRR (peptide **13**). However, introduction of a *cis* C^{β}-methyl substituent on proline 5, VPPPP(CH_3)PPRRR (peptide **14**), restored the binding potency (K_d = 16.8 ± 0.7 μM), with a slight affinity enhancement when compared to peptide **12** (Fig. 6 and Table 2). Surprisingly, none of the other *cis* C^{β}-substituted monomeric peptides (peptides **15**–**19**) were able to interact with detectable affinity to the Grb2 protein (Table 2).

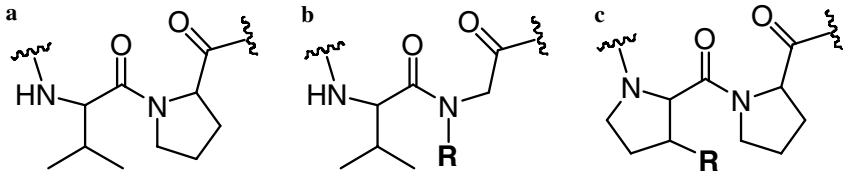

Figure 3. (a) The Val5-Pro6 pair of the Sos wild-type decapeptide and corresponding structures for (b) the peptoid ligands developed by Nguyen et al.,[10] and for (c) the C^{β}-substituted Pro5 peptides described herein.

Table 1. *N*-Boc or *N*-Fmoc *cis* C^{β}-substituted-L-prolines used for the synthesis of the VPPPVPPRRR-derived peptides

C^{β}-substituted proline	Substituent R	Protecting group P	Compound	Ref
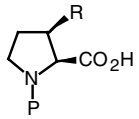	H	Boc	**5**	
	CH_3	Fmoc	**6**	22
	$CH(CH_3)_2$	Fmoc	**7**	26, 28
	$CH_2OCH_2C_6H_5$	Boc	**8**	27
	CH_2SCH_3	Fmoc	**9**	22, 23
	CH_2CN	Fmoc	**10**	25, 27
	$CH_2SO_2C_6H_5$	Boc	**11**	26

2.3. Far-UV CD analysis

Far-UV CD spectra were recorded to monitor the conformational changes on the PPII conformation induced by substitution of Val5 by various *cis* C^{β}-substituted-L-prolines of the active peptides. CD spectrum of VPPPPPPRRR (peptide **13**) revealed a characteristic PPII signature with a strong minimum at 201 nm and a weak maximum at 227 nm.[26] The absence of maximum at 227 nm for VPPPVPPRRR (peptide **12**) suggests that the PPII conformation was less pronounced (Fig. 7), although still present. Far-UV CD spectrum of VPPPP(CH_3)PPRRR (peptide **14**) is almost superimposable with the spectrum of peptide **13**.

2.4. Peptide optimization

To evaluate the effects of the N- and C-terminal charges on the binding to Grb2, the *N*-acetyl, C-carboxamide analogue of peptide **12** was prepared (peptide **20**). These two modifications induced a 10-fold increase in the binding potency ($K_d = 3.7 \pm 0.2$ μM), when compared to peptide **12** (Table 2). Then, peptide dimerization was explored, as peptide dimers, which allow simultaneous interaction with both Grb2-SH3 domains, have presented significant increase in binding potency.[13,25] The affinity of dimeric peptide **21**, obtained from the best monomeric ligand (peptide **14**), was determined by fluorescence spectroscopy and ITC. Compared to peptides **12** and **14**, peptide **21** presented a dramatic increase in affinity. By fluorescence, the K_d of **21** was estimated between 9 and 520 nM, the dissociation constant being quantitatively determined by ITC as being in the nanomolar range, $K_d = 68 \pm 5$ nM (Fig. 8).

3. Discussion

The interacting surface (400 $Å^2$) delineated within each Grb2-SH3 domain plays a crucial role in the modulation of the MAPK-dependent intracellular mechanisms. The Sos decapeptide, VPPPVPPRRR, that contains the specific PXXP signature of SH3 binding motifs (where X is any amino acid), interacts within three grooves (Fig. 2) located at either surface of the N- or C-terminal domains of the Grb2 protein. Binding mode of this peptide belongs to the type II, that is, with residues Pro2 and Pro3 fitting within the first shallow pocket, while residues Val5 and Pro6 are located within the second, and the charged Arg8 residue interacting with an aspartate residue of the third pocket (Asp33 and Asp190 for the Grb2 N-terminal and C-terminal SH3 domains, respectively). Briefly, when the basic residues are located at the N-terminus of the PPII peptide, the latter adopts a type-I binding mode, whereas it is considered as a type-II binding mode when the basic residues are located at the C-terminus.[27,28] The second pocket is an aromatic-rich region delimited by residues Phe9, Trp36, Pro49 and Tyr52 for the N-terminal Grb2-SH3 domain,[8] and residues Phe167, Trp193, Pro206 and Tyr209 for the C-terminal domain.[29] The third pocket confers specificity to the complex.[5]

In their elegant work, Nguyen et al.,[10] have shown that: (i) prolines of the central **PXXP** sequence could actually

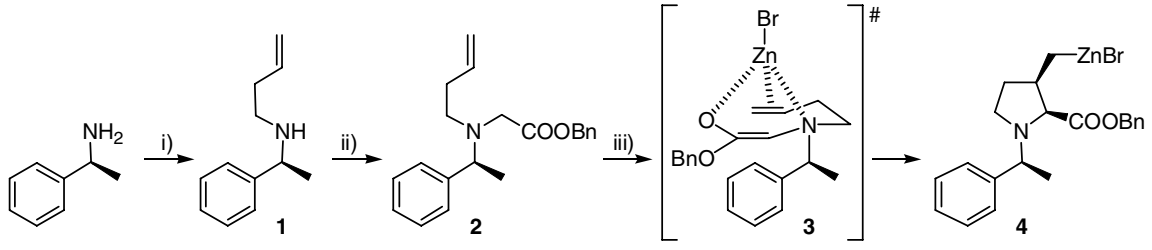

Figure 4. Amino-zinc-ene-enolate carbometallation reaction. Reagents and conditions: (i) 4-bromobutene, K_2CO_3, NaI, DMF, 80 °C; (ii) benzyl bromoacetate, K_2CO_3, anhydrous THF/DMPU, rt; (iii) anhydrous diethyl ether, LDA (−78 °C), $ZnBr_2$ (−78 °C to rt).

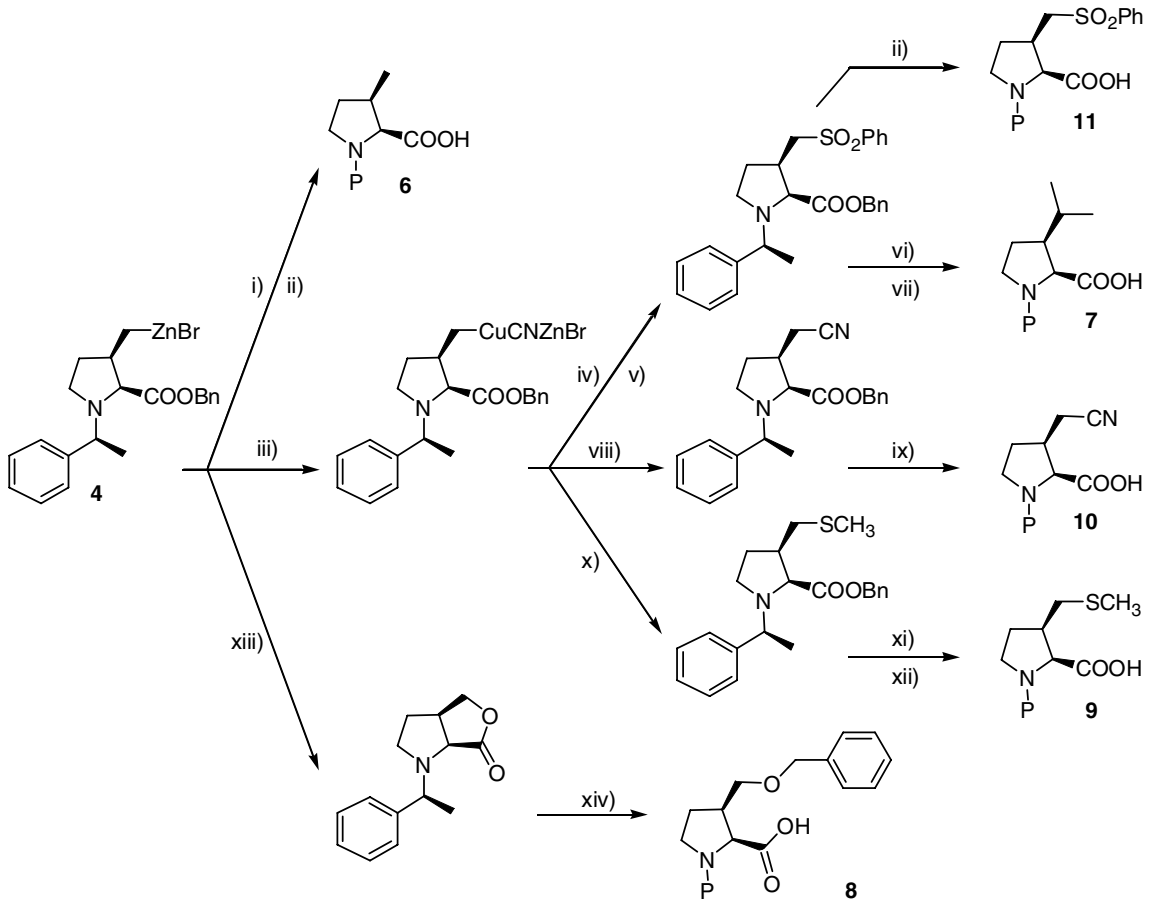

Figure 5. Synthesis of the *cis* C^{β}-substituted-L-prolines **6**–**11**. Reagents and conditions: (i) NH_4Cl, H_2O; (ii) H_2, Pd/C, Boc_2O, MeOH or Fmoc-*O*-succinimide, pH 9; (iii) CuCN/2LiCl; (iv) $PhSSO_2Ph$; (v) CH_2Cl_2, THF, mCpBA; (vi) THF/DMPU, −78 °C, LDA, CH_3I and then LDEA, CH_3I; (vii) MeOH, Na/Hg, KH_2PO_4 and then H_2, Pd/C, Boc_2O, MeOH; (viii) TsCN; (ix) H_2, Pd/C, Boc_2O, MeOH; (x) $CH_3SSO_2CH_3$ at 0 °C; (xi) VocCl, $(CH_2Cl)_2$; (xii) HCl gaz, dioxane and then Boc_2O or Fmoc-*O*-succinimide; (xiii) O_2; (xiv) H_2, Pd/C, Boc_2O, MeOH and then excess of KOH, BnBr.

Table 2. K_d measurements of synthetic peptides **12**–**21** for Grb2-SH3 domains by intrinsic tryptophane fluorescence spectroscopy

Synthetic peptide	Compound	K_d (μM)
H-VPPP**V**PPRRR-OH	**12**	38.15
H-VPPP**P**PPRRR-OH	**13**	nb
H-VPPP**P**(CH_3)PPRRR-OH	**14**	11.60
H-VPPP**P**($CH(CH_3)_2$)PPRRR-OH	**15**	nb
H-VPPP**P**(CH_2OH)PPRRR-OH	**16**	nb
H-VPPP**P**(CH_2SOCH_3)PPRRR-OH	**17**	nb[a]
H-VPPP**P**(CH_2COOH)PPRRR-OH	**18**	nb[b]
H-VPPP**P**($CH_2SO_2C_6H_5$)PPRRR-OH	**19**	nb
Ac-VPPP**V**PPRRR-NH_2	**20**	3.67
(Ac-VPPP**P**(CH_3)PPRRR)$_2$K-NH_2	**21**	<0.52

Proline substituent is oxidized into sulfoxide (a) or carboxylic acid (b), respectively.
nb, no binding.

be replaced by non-natural N-substituted residues without hampering complex formation and (ii) substitution of Val5 in the VP**PPVP**PRRR decapeptide by sarcosine was associated to a lower affinity for Grb2. Replacement of Pro6, the last proline in the PXX**P** sequence, by, for example, *N*-(*S*)-phenylethylglycine within the Sos decapeptide, was found to noticeably enhance (≈100-fold) the affinity for the isolated N-terminal Grb2-SH3 domain. The authors suggested that proline was not chosen during evolution for its conformation properties, but because proline was the only naturally occurring N-substituted amino acid.[10] Nguyen et al. also hypothesized that N-substitution of the penultimate residue **X** in the PX(**X** = **Val**)P sequence could not be tolerated by the SH3 domains, due to the narrowness of second SH3 groove (25 Å long and 10 Å wide).[10] Apparently in contradiction with this enthalpy-driven hypothesis, Ferreon et al.[30] proposed an entropy-driven hypothesis for the Grb2/Sos interaction, since they showed that decreased affinities for SH3 domain were observed when the PPII conformation of Sos-derived peptides was destabilized.

In the present study, far-UV CD spectrum of the VPPPPPPRRR peptide **13** (substitution of Val5 by Pro5) unambiguously showed that the PPII concentration is increased compared to that observed for VPPPVPPRRR. However, peptide **13** has no affinity for Grb2. Inspection of the published NMR structure of the N-terminal Grb2-SH3 domain/VPPPVPPRRR (PDB code: 1GBQ)[8] shows the conformation of the bound peptide and yields for Val5 the following values: $\omega = -177°$, $\phi = -69°$, $\psi = 139°$ with the N-C^{α}-C^{β}-$C^{\gamma 2}$ torsion angle equal to −33°. These values correspond

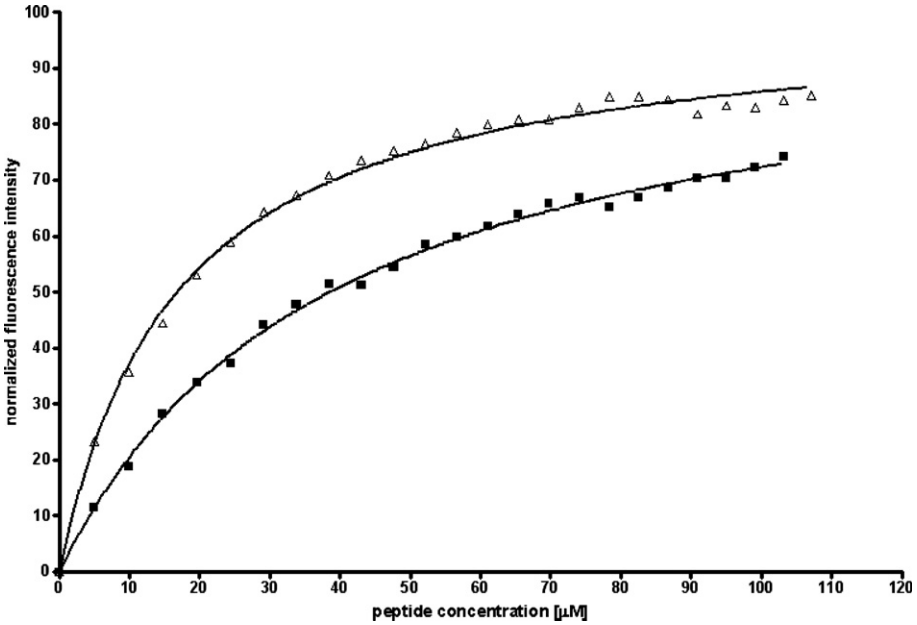

Figure 6. Fluorescence change of Grb2 by (■) peptide **12** and (△) peptide **14** binding. Experimental datapoints have been fitted using a Monte Carlo-based program.[34]

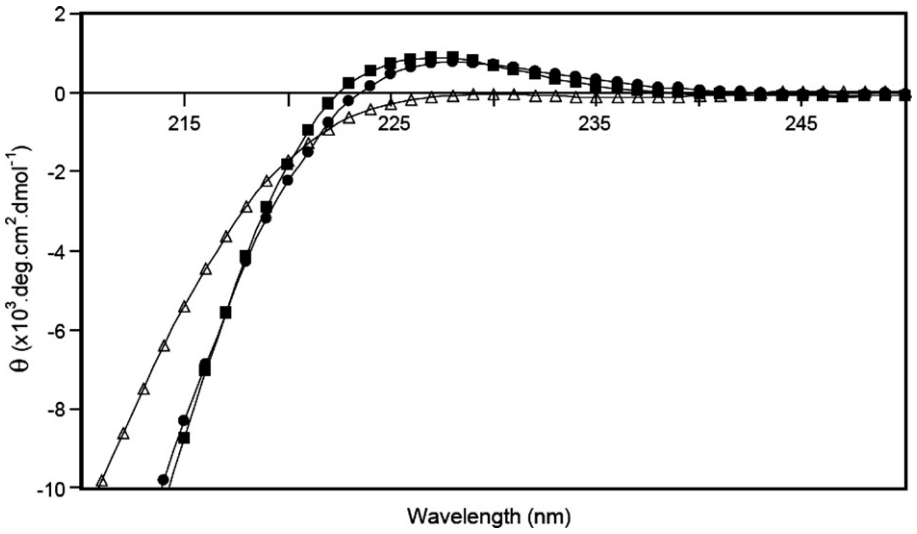

Figure 7. CD spectra of derivatives **12** (△), **13** (■) and **14** (●) recorded at 5 °C. For each peptide, concentration sample was 300 µM in phosphate buffer 15 mM, pH 7, NaCl 40 mM.

to typical angles for a proline within a PPII structure, with an up-puckering ($\chi 1 = -27°$) for the pyrrolidine ring.[31] Furthermore, the γ1 and γ2 methyls of Val5 in the decapeptide interact strongly with the hydrophobic residues located in the second pocket (distances measured between $C^{\gamma 1}$ and Pro49 C^{β}; Pro49 C^{γ}; Phe9 C^{ζ}; Trp36 $C^{\eta 2}$; Trp36 $C^{\zeta 2}$ are 3.75, 3.53, 3.91, 3.42, 3.61 Å, respectively, and distances measured between $C^{\gamma 2}$ and Tyr52 C^{ζ}; Tyr52 $C^{\varepsilon 1}$; Phe9 $C^{\varepsilon 1}$ are 3.90, 3.54, 3.61 Å, respectively, Fig. 2).

Herein, we speculated that a C^{β}-substituted Pro5 (**X**) followed by a Pro6 residue in the P**XXP** sequence could constitute an amino acid combination comparable to the sequential C^{α}- and N-substituted residues, which were described as the prominent feature of SH3 ligands.[14] In the present study, *cis*-configuration of the C^{β}-substituent on the proline scaffold was chosen to explore the external face of the second groove. *trans*-Configuration with bulky substituents might lead to steric clashes with Phe9, Trp36 and Pro49 of the N-terminal domain or Phe167, Trp193 and Pro206 of the C-terminal domain, respectively. Among compounds **14**–**19**, only peptide **14**, bearing a *cis* C^{β}-methyl-L-proline, $P(CH_3)$, exhibits an enhanced affinity for the Grb2 protein. This improvement remains marginal (factor 3), when compared to the wild-type peptide. Unexpectedly, the phenyl-containing peptide **19** has no affinity at all for Grb2, despite the presence of numerous aromatic residues in the second SH3 pocket

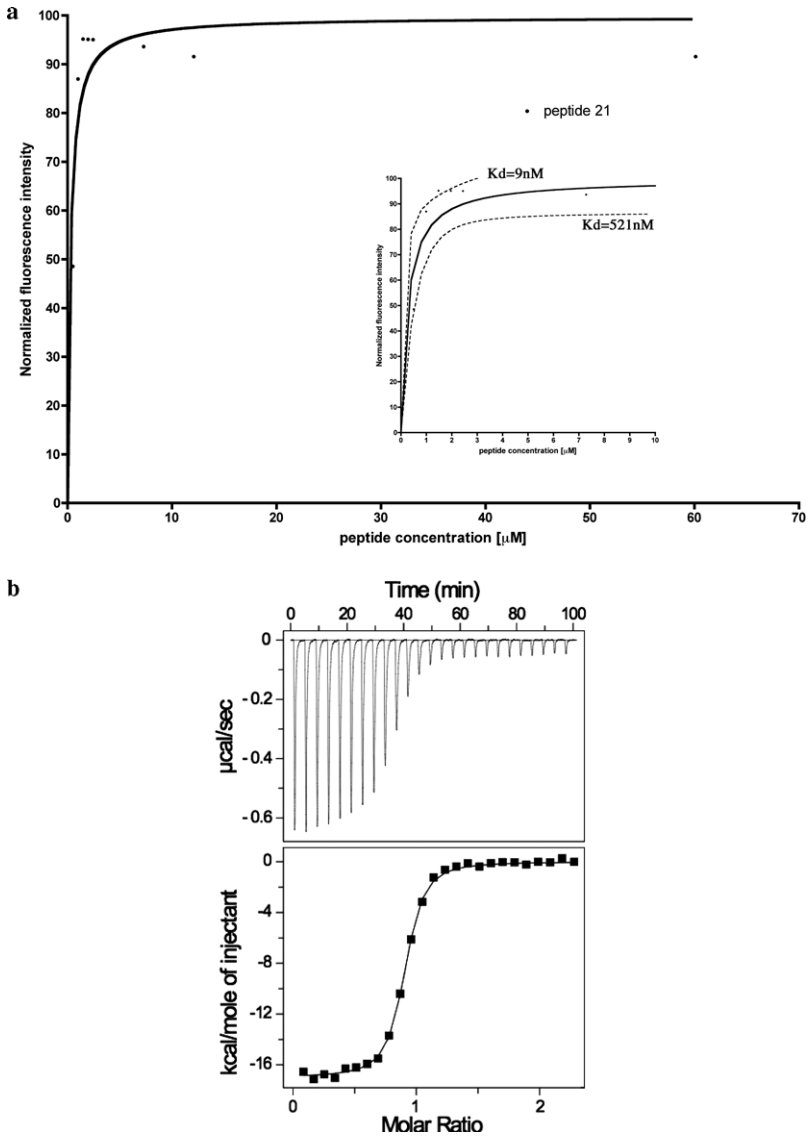

Figure 8. Grb2-binding curve obtained at 18 °C with increasing concentrations of peptide **21**. Dissociation constants were measured either by (a) fluorescence spectroscopy (0,009 μM < K_d < 0.520 μM) or (b) by ITC (K_d = 68 ± 5 nM, stoichiometry N = 1).

and the high affinity of some N-alkylated peptoids, described by Nguyen et al.[10] Compared to peptide **13**, the affinity enhancement obtained for the peptide **14** (incorporating a *cis* C^{β}-methyl-L-proline) might be promoted by local hydrophobic interactions involving the methyl substituent. Indeed, the CD spectrum of peptide **14** is almost completely superimposable with the CD spectrum of peptide **13**, proving that the methyl substituent neither increases nor decreases significantly the PPII conformation (Fig. 7). Minimizations of the complex containing peptide **14** and the N-terminal Grb2-SH3 domain have been carried out to correlate observed affinities and ligand/protein interactions. Interestingly, each of the two P(CH_3) ring conformations (up- or down-puckering) was found to share specific structural homologies with the Val5 residue of the wild-type sequence (Fig. 9). Indeed, superimposing the N, C^{α}, C^{β}, $C^{\gamma 2}$, C' and O atoms of Val5 (coordinates taken from the minimized 1GBQ structure[8]) with the corresponding N, C^{α}, C^{β}, C^{γ}, C' and O atoms of the up-puckered and down-puckered P(CH_3) ring gave a rms value of 0.26 and 0.65 Å, respectively. These results are to be related to the previous finding that Val5 torsion angles of the bound peptide are almost identical to those found in *trans* up-puckered prolines. Thus, the C^{γ}-methylene group of an up-puckered Pro5 could nicely mimic the valine $C^{\gamma 2}$-methyl of the wild-type ligand and allows the corresponding hydrophobic interactions with the protein to take place. However, no new hydrophobic interaction was detected between the C^{γ}-methylene group of the up-puckered 3-substituted Pro5 and the protein when compared with those detected in the wild-type complex, that is, between the γ2-methyl of Val5 and the protein. In contrast, based on these structural alignments, the *cis* C^{β}-methyl group of the P(CH_3) residue is found 2.01 Å away from the valine $C^{\gamma 1}$-methyl for the up-puckering form of Pro5 and only 0.54 Å away for the down conformation (Fig. 9). It is thus highlighted that the *cis* C^{β}-methyl

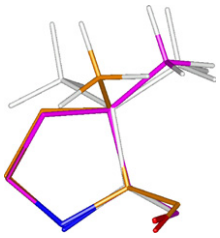

Figure 9. Superimposition of the down-puckered (purple) and the up-puckered (orange) *cis* 3-methylproline in position 5 of the peptide ligand with the Val5 (in white) of the wild-type peptide after minimization of the complexes.

substituent of Pro5 could fairly mimic the wild-type valine $C^{\gamma 1}$-methyl, provided that the pyrrolidine ring adopts a down-puckered conformation. In conclusion, the *cis* 3-methylproline residue fits well with Val5 residue and therefore allows the peptide to be well accommodated within the binding pocket. The additional C^{δ}-methylene group in the pyrrolidine ring is oriented away from the protein surface and therefore does not contribute significantly to van der Waals interactions with the protein.

For peptide optimization the N- and C-terminal charges of peptide **12** were first removed, since the decapeptide of Sos is included in a protein sequence. The resulting peptide **20** presented a 10-fold increase in affinity for Grb2. Both peptides **12** and **20** exhibited the same CD spectrum profile suggesting that the different affinities are only related to electrostatic effects (data not shown). Then, with these N- and C-terminal modifications, the best monomeric ligand, peptide **14**, has been dimerized with a lysine linker, as previously published.[13,25] The dimer dissociation constant was too tight to be measured by fluorescence and was therefore quantified by ITC ($K_d = 68 \pm 5$ nM). Interestingly, ITC analysis demonstrated a stoechiometry very close to $N = 1$ for the Grb2/ligand complex, in good agreement with the model where one dimeric ligand simultaneously interacts with both Grb2-SH3 domains (Fig. 8).

Thus, the modest three-fold affinity gain achieved by replacement of Val5 combined with neutralization of the N- and C-terminal charges, as carboxamide and N-acetyl forms, and finally dimerization leads to one of the most potent Grb2-SH3-domain ligand described so far with a 560-fold increase of affinity when compared to the wild-type monomer H-VPPPVPPRRR-OH. To date, the best ligands reported in the literature were a peptide dimer[13,25] and a peptoid[10,14] and gave a 450- and a 125-fold affinity increase, respectively (referring to the wild-type monomer). Interestingly, our peptide might be further optimized by C^{γ} pyrrolidine ring functionalization. C^{δ} or *trans* C^{β} bulky substituents are precluded because of steric hindrance within both the N- and C-terminal domains of Grb2. However, introduction of a *trans* C^{β}-methyl could be beneficial, since it could mimic the $C^{\gamma 1}$ of Val5 in an up-puckered state of the pyrrolidine ring, this conformation being also required for observing the Pro5 C^{γ}–Val5 $C^{\gamma 2}$ structural homology.

4. Conclusion

We report the synthesis of new Grb2 ligands starting from the Sos decapeptide, VPPPVPPRRR substituted in position 5. The key residue valine 5 has been replaced by various *cis* C^{β}-substituted prolines. Data clearly show that PPII conformation of the substituted peptide is stabilized by introduction of an additional pyrrolidine ring in position 5. But, an increase of PPII conformation is not sufficient to yield high affinity Grb2 ligand. However, an additional *cis* C^{β}-methyl on the pyrrolidine ring slightly increases the binding potency to Grb2 of the resulting peptide by mimicking partially the $C^{\gamma 1}$-methyl of the valine 5. Other *cis* C^{β}-proline substituents, such as phenyl, substituted-phenyl, bulky aliphatic groups and polar chains, unexpectedly led to complete loss of binding potency for Grb2. Finally, the *cis* C^{β}-methyl-proline 5, *N*-acetylated, C-carboxamide dimer **21** yielded a 560-fold affinity enhancement compared to the wild-type VPPPVPPRRR sequence. Interestingly, this compound is one of the most potent Grb2 SH3-domain peptide ligands described so far when compared to the wild-type monomer H-VPPPVPPRRR-OH. Indeed, the best peptide ligands reported in the literature are a peptide dimer[13,25] and a peptoid[10,14] that gave a 450- or a 125-fold affinity increase, respectively (referring to the wild-type monomer). This study shows that C^{β}-substituted proline may constitute a new alternative for PPII ligands, combining entropy and enthalpy beneficial effects.

5. Experimental

5.1. Chemistry

Automatic peptide syntheses were achieved on a ABI 433 A peptide synthesizer (Applied Biosystems, Foster City, USA). Boc-protected natural amino acids, HBTU, Arg(Tos), preloaded PAM resin (substitution 0.57 mmol/g) and MBHA resin (substitution 1.26 mmol/g) were purchased from Senn Chemicals Int. (Cachan, France). Solutions in NMP of DCC (1.0 M), HOBt (1.0 M) and DMSO were obtained from Applied Biosystems (Courtaboeuf, France). NMP, DIEA and dichloromethane were purchased from SDS (Peypin, France). Boc or Fmoc N-protected modified prolines **6–11** were prepared according to already reported procedures.[18–24] otherwise stated 10 equivalents of the protected-amino acids was used. Peptides were cleaved from the support by HF, as already described.[32] After lyophilisation, peptides were purified by RP-HPLC with appropriate gradient (30 min) of solvent B (60% acetonitrile in 0.1% (v/v) TFA/H_2O). Preparative RP-HPLC was achieved on a Dionex HPLC system (Dionex P580 Pump, Dionex AD25 Absorbance Detector at 200 nm, Dionex 4400 Integrator), with a flow rate of 6 ml/min, using a SymmetryPrep® C_8 RP-HPLC column (Waters 7.8 mm × 300 mm, 7 μm particle size, 300 Å pore size). Analytical RP-HPLC was achieved on a Waters HPLC system (Waters 600 Pump and Controller, Waters 2487 Dual λ Detector, Waters 746 Data Module), with a flow-rate of 1.5 mL/min,

using a C_8 RP-HPLC column (Waters 4.6 mm × 300 mm, 5 μm particle size, 300 Å pore size). MALDI-TOF spectra were recorded with a PerSeptive Biosystems Voyager Elite mass spectrometer (Applied Biosystems Framingham, USA).

5.1.1. Synthesis of peptides 12 and 13. Peptides **12** and **13** were obtained starting from a Boc-Arg(Tos)-preloaded PAM resin (0.1 mmol).

Peptide **12**: RP-HPLC, R_t = 10.3 min (30 min gradient from 9% to 48% solvent B). MALDI-TOF ($M+H^+$) 1170.7 (calcd 1169.7). Peptide **13**: RP-HPLC, R_t = 12.7 min (30 min gradient from 0% to 24% solvent B). MALDI-TOF ($M+H^+$) 1168.9 (calcd 1167.7).

5.1.2. Synthesis of peptides 14–19. Peptides **14**–**19** were obtained starting from a Boc-Arg(Tos)-preloaded PAM resin (0.1 mmol). The *cis* C^{β}-substituted Pro5 and the next Pro4 residues were manually coupled, 5 equiv for the substituted Pro5 and 10 equiv for Pro4, respectively, the activation being performed with HBTU in the presence of DIEA in NMP. The Boc or Fmoc protecting groups were removed from the modified prolines with either TFA (20% v/v in dichloromethane) or piperidine (20% v/v in dichloromethane), respectively.

Peptide **14**: RP-HPLC, R_t = 18.7 min (30 min gradient from 0% to 18% solvent B). MALDI-TOF ($M+H^+$) 1182.9 (calcd 1181.7). Peptide **15**: RP-HPLC, R_t = 11.3 min (30 min gradient 0–18% solvent B). MALDI-TOF ($M+H^+$) 1210.5 (calcd 1209.8). Peptide **16**: RP-HPLC, R_t = 16.5 min (30 min gradient 0–18% solvent B). MALDI-TOF ($M+H^+$) 1198.8 (calcd 1197.7). Peptide **17**: RP-HPLC, R_t = 20.8 min (gradient 0–30% of solvent B over 30 min). MALDI-TOF ($M+H^+$) 1244.9 (calcd 1243.7). Peptide **18**: RP-HPLC, R_t = 19.2 min (30 min gradient 0–18% solvent B). MALDI-TOF (M^+) 1225.3 (calcd 1225.7). Peptide **19**: RP-HPLC, R_t = 21.5 min (30 min gradient 0–18% solvent B). MALDI-TOF ($M+H^+$) 1322.6 (calcd 1321.7).

5.1.3. Synthesis of the *N*-acetylated and C-carboxamide peptide monomer 20. Peptide **20** was obtained starting from a MBHA resin. Fmoc *cis* C^{β}-methyl proline was coupled as described for peptide **14**. After removal of the last Boc-protecting group, the amino terminal was acetylated by an excess of acetic anhydride. RP-HPLC, R_t = 15.9 min (30 min gradient 6–30% solvent B). MALDI-TOF ($M+H^+$) 1211.9 (calcd 1210.7).

5.1.4. Synthesis of the *N*-acetylated and C-carboxamide peptide dimer 21. Peptide **21** was obtained starting from a MBHA resin preloaded with Boc-Lys(Fmoc)-OH (0.1 mmol). After sequential removal of the Boc and the Fmoc protecting groups, both amino functions of the lysine residue were simultaneously elongated by double couplings (each time 10 equiv). Fmoc *cis* C^{β}-methyl proline (residue 5) as well as the following amino acid (Pro4) were introduced manually by single coupling (5 and 10 equiv, respectively) after activation with HBTU in the presence of DIEA in NMP. After removal of the last Boc-protecting group, the amino terminal was acetylated by an excess of acetic anhydride RP-HPLC, R_t = 13.2 min (40 min gradient 0–60% solvent B). MALDI-TOF ($M+H^+$) 2557.1 (calcd 2556.6).

5.2. Modelling

Calculations were performed on Silicon Graphics O2 workstations, using Discover software (Accelrys, Inc, San Diego, USA) and cff91 forcefield. The complex between the N-terminal Grb2-SH3 domain and the Ac-VPPPVPPRRR-NH_2 peptide was obtained from the Protein Data Bank (PDB code: 1GBQ)[8] and was used in all calculations. Visualisation and chemical modifications of the PDB structure were carried out using Insight II and Biopolymer (Accelrys). A minimization protocol was applied on the wild-type complex as well as on the complex incorporating peptide **14**, by considering separately an up- or down-puckering of the $P(CH_3)$. Nonbond interactions were calculated using a 8 Å cutoff. The electrostatic potential was calculated in vacuo with a distance-dependent dielectric $\varepsilon = 4r$. The minimization protocol consisted of four stages in which constraints on atom positions were gradually removed: (i) relaxation of peptide ligand side chains, (ii) relaxation of the whole peptide, (iii) relaxation of the entire complex except the protein backbone and (iv) relaxation of the entire complex. Each minimization step consisted of a total of 5000 iterations (10,000 for the final one) using steepest descent and conjugate gradient algorithms until the gradient was less than 0.001 kcal mol^{-1} $Å^{-1}$.

5.3. Fluorescence-based binding assays

The recombinant Grb2 protein has been produced and purified according to already reported protocol.[33] Affinity of the peptides for the recombinant Grb2 protein was evaluated using fluorescence-based titration assays. Experiments were conducted at 18 °C in a stirred 1 cm pathlength cell using a Jasco FP-6200 spectrofluorimeter (Jasco, Essex, United Kingdom). Excitation and fluorescence emission were monitored at 280 and 350 nm, respectively. In all cases, concentration of Grb2 was kept at 1 μM in 50 mM of Tris buffer adjusted at pH 8.0. Peptide concentrations varied typically from 50 nM to 250 μM. Dissociation constants K_d were determined by monitoring changes of fluorescence upon addition of the peptide at defined concentrations. Experimental curves were fitted using the Monte Carlo-based MC-Fit program.[34] Dissociation constants (K_d) were calculated according to the following equation: $F_b = (K_d + P + L \pm ((K_d + P + L)^2 - 4PL)^{1/2})/2P$, where P and L are the protein and peptide concentrations, respectively, and F_b the fraction of the bound peptide. For high affinities, $K_d \approx P$.

5.4. Isothermal titration calorimetry

ITC experiments were carried out on a VP-ITC isothermal titration calorimeter (Microcal, Northampton, USA) at 18 °C. The same buffer (50 mM Tris, pH 8.0) was used for compound **21** and Grb2. Grb2 concentration was determined by UV spectroscopy and initially adjusted at 10.4 μM in the microcalorimeter cell (2.1

mL). A 5 or 10 μL volume of peptide **21** (stock solution at 125 μM) was added from a computer-controlled 300 μL microsyringe at intervals of 4 min. Heat dilution of the peptide was taken into account from peaks measured after full saturation of Grb2 by the peptide. A theoretical titration curve was fitted to the experimental data using the ORIGIN software (Microcal). This software uses the relationship between the heat generated by each injection and ΔH° (enthalpy change in kcal $mole^{-1}$), K_A (association binding constant in M^{-1}), n (number of binding sites per monomer), total protein concentration and free and total ligand concentrations.

5.5. Circular dichroism

CD spectra were acquired on a Jobin Yvon CD6 dichroism spectropolarimeter at 5 °C using a 1 mm pathlength quartz cell. Spectra were recorded from 185 to 260 nm using a 300 μM solution of peptide in phosphate buffer 15 mM, pH 7, NaCl 40 mM, and were averaged over four scans after baseline correction.

Acknowledgments

We are grateful to Dr. Fabienne Burlina for mass spectra analysis and to Vanessa Point for experimental assistance. We are also grateful to Drs. S. Fermandjian and L. Zargarian (CNRS-UMR 8113, Institut Gustave Roussy, Villejuif) for dichroism experiments.

References and notes

1. Olson, M. F.; Marais, R. *Semin. Immunol.* **2000**, *12*, 63.
2. Schlessinger, J. *Cell* **2000**, *103*, 63.
3. Kolch, W. *Biochem. J.* **2000**, *351*, 289.
4. Midgley, R. S.; Kerr, D. J. *Crit. Rev. Oncol. Hematol.* **2002**, *44*, 63.
5. Kay, B. N.; Williamson, M. P.; Sudol, M. *FASEB J.* **2000**, *14*, 231.
6. Simon, J. A.; Schreiber, S. L. *Chem. Biol.* **1995**, *2*, 53.
7. Goudreau, N.; Cornille, F.; Duchesne, M.; Parker, F.; Tocqué, B.; Garbay, C.; Roques, B. P. *Struct. Biol.* **1994**, *1*, 898.
8. Wittekind, M.; Mapelli, C.; Lee, V.; Goldfarb, V.; Friedrichs, M. S.; Meyers, C. A.; Mueller, L. *J. Mol. Biol.* **1997**, *267*, 933.
9. Williamson, M. P. *Biochem. J.* **1994**, *297*, 249.
10. Nguyen, J. T.; Turck, C. W.; Cohen, F. E.; Zuckermann, R. N.; Lim, W. A. *Science* **1998**, *282*, 2088.
11. Dalgarno, D. C.; Botfield, M. C.; Rickles, R. J. *Biopolymers* **1997**, *43*, 383.
12. Robinson, J. M.; Cobb, M. H. *Curr. Opin. Cell Biol.* **1997**, *9*, 180.
13. Cussac, D.; Vidal, M.; Leprince, C.; Liu, W.-Q.; Cornille, F.; Tiraboschi, G.; Roques, B. P.; Garbay, C. *FASEB J.* **1999**, *13*, 31.
14. Nguyen, J. T.; Porter, M.; Amoui, M.; Miller, W. T.; Zuckermann, R. N.; Lim, A. W. *Chem. Biol.* **2000**, *7*, 463.
15. Smithgall, T. E. *J. Pharmacol. Toxicol. Methods* **1995**, *34*, 125.
16. Ladbury, J. E.; Arold, S. *Chem. Biol.* **2000**, *7*, R3.
17. Kärkkäinen, S.; Hiipakka, M.; Wang, J.-H.; Kleino, I.; Vähä-Jaakkola, M.; Renkema, G. H.; Liss, M.; Wagner, R.; Saksela, K. *EMBO Reports* **2005**, *7*, 186.
18. Karoyan, P.; Chassaing, G. *Tetrahedron Lett.* **1997**, *38*, 85.
19. Karoyan, P.; Chassaing, G. *Tetrahedron: Asymmetry* **1997**, *8*, 2025.
20. Karoyan, P.; Triolo, A.; Nanncini, R.; Giannotti, D.; Altamura, M.; Chassaing, G.; Perrotta, E. *Tetrahedron Lett.* **1999**, *40*, 71.
21. Karoyan, P.; Chassaing, G. *Tetrahedron Lett.* **2002**, *43*, 253.
22. Karoyan, P.; Quancard, J.; Vaissermann, J.; Chassaing, G. *J. Org. Chem.* **2003**, *68*, 2256.
23. Quancard, J.; Labonne, A.; Jacquot, Y.; Chassaing, G.; Lavielle, S.; Karoyan, P. *J. Org. Chem.* **2004**, *69*, 7940.
24. Karoyan, P.; Chassaing, G. *Tetrahedron Lett.* **2002**, *43*, 1221.
25. Vidal, M.; Liu, W.-Q.; Lenoir, C.; Salzmann, J.; Gresh, N.; Garbay, C. *Biochemistry* **2004**, *43*, 7336.
26. Kelly, M. A.; Chellgren, B. W.; Rucker, A. L.; Troutman, J. M.; Fried, M. G.; Miller, A.- F.; Creamer, T. P. *Biochemistry* **2001**, *40*, 14376.
27. Mayer, B. J. *J. Cell Sci.* **2001**, *26*, 1253.
28. Feng, S.; Chen, J. K.; Yu, H.; Simon, J. A.; Schreiber, S. L. *Science* **1994**, *266*, 1241.
29. Kohda, D.; Terasawa, H.; Ichikawa, S.; Ogura, K.; Hatanaka, H.; Mandiyan, V.; Ullrich, A.; Schlessinger, J.; Inagaki, F. *Structure* **1994**, *2*, 1029.
30. Ferreon, J. C.; Hilser, V. J. *Protein Sci.* **2003**, *12*, 447.
31. Markley, J. L.; Bax, A.; Arata, Y.; Hilbers, C. W.; Kaptein, R.; Sykes, B. D.; Wright, P. E.; Wuthrich, K. *J. Mol. Biol.* **1998**, *280*, 933.
32. Josien, H.; Lavielle, S.; Brunissen, A.; Saffroy, M.; Torrens, Y.; Beaujouan, J. C.; Glowinski, J.; Chassaing, G. *J. Med. Chem.* **1994**, *37*, 1586.
33. Guilloteau, J. P.; Fromage, N.; Rieskautt, M.; Reboul, S.; Bocquet, D.; Dubois, H.; Faucher, D.; Colonna, C.; Ducruix, A.; Becquart, J. *Protein Struct. Funct. Genet.* **1996**, *25*, 112.
34. Dardel, F. *Comput. Appl. Biosci.* **1994**, *10*, 273.